Journal of
Biomedical Systems & Emerging Technologies

Research Article Open Access

Measurement and Consideration of the Breakdown Voltage in a Micro Gap ESD

Ishigami S*, Kawamata K and Minegishi S

Faculty of Engineering, Tohoku Gakuin University, Japan

Abstract

We examined that the physical processes of an electrostatic discharge occurring on the applied voltage of less than 330 V and at gap lengths of several micrometers by measuring the discharge current and electric fields. As a result, it was confirmed that the conventional Paschen's law cannot be applied to the characteristics of discharges on the applied voltage of less than 330 V in the gap lengths of less than 4 μm in both cases of approaching electrode and fixed electrode. The breakdown process was explained in terms of the equation describes the relationship between high density electrons and electric-field strength that is applied for high electric-field. The proposed equation expressed both the conventional Paschen's law and the breakdown process below the Paschen minimum.

Keywords: Micro gap discharge; Electrostatic Discharge (ESD); Breakdown voltage; Paschen's law

Introduction

The immunity of recent electronic equipment such as microcomputers to fast transient fields tends to be degraded because the equipment runs faster and with lower power-consumption than the past. Electrostatic Discharge (ESD) is one of the serious noise sources to electronic equipment. An ESD generates a fast-transient field and its spectrum is broadly distributed over the frequency range up to SHF band [1]. It is reported that fields of the low-voltage ESD (less than about 600 V) have faster rise time compared with the high-voltage ESD [2].

Moreover, a characteristic of electromagnetic field in a case of an approaching electrode which simulates an actual ESD event differs from those of fixed electrodes [2]. Therefore, the ESD fields in the case of the approaching electrode with a low applied voltage should be measured to examine the malfunction of electronic equipment. In Kawamata et al. [3], discharge waveforms of an approaching electrode are observed by using a transmission line and a waveform digitizer. In the reference, applied voltages are from 400 V to 1300 V, of which voltages are in the range of application for the Paschen's law. It is known that discharges occur on the applied voltage below 330 V in a case of approaching electrode. The applied voltage of 330 V is the minimum breakdown voltage in air (the Paschen minimum). Bock and Hartnagel [4] reported that the discharge occurs on below 330 V for fixed electrodes with about 0.6 μm gap length. It is also reported that the discharge below the Paschen minimum is observed in various types of gas (SF6, N2, Air, and others) and under various pressure conditions [5]. However, the physical breakdown processes at such voltage are not well elucidated.

In this paper, the discharge currents and the electric fields caused by an ESD are measured with the gap length of a few micrometers at applied voltages less than 330 V. The purpose of this paper is to contribute to the understanding of the physical processes of the discharge at less than the Paschen minimum.

Measurement of Discharge Current and Electric Field

Setup for measurements

Equipment for measuring an electric field and a discharge current mainly consists of a discharge apparatus, a current sensor, a waveform measuring instrument, and an electric-field sensor (a monopole antenna) as shown in Figure 1. The discharge apparatus consists of a DC high-voltage source, a capacitor, and discharge electrodes that are made from copper with a diameter of 6.0 mm. The tip of the electrodes is semi-sphere in shape. The diameter of the electrodes and the tip-shape of the electrodes were selected as generating a uniform electric field between the electrodes. The electrode surface was polished by liquid abrasive with a particle size of below 1 μm. A discharge occurs between these electrodes. One electrode for grounding is movable by using a piezo actuator to adjust a gap length precisely. The waveform measuring instrument is composed of a delay-line, a broadband amplifier with a bandwidth of 5.1 GHz, and a 4.5 GHz-bandwidth waveform digitizer (Tektronix SCD5000). The value of the capacitor (150 pF) was determined by a stray capacitance of human ESD, which is adopted by an ESD gun for immunity tests. The value of the resistor (30 Ω) was determined as the time constant 4.5 ns (30 Ω x 150 pF) was intended to be smaller than 10 ns that is the measuring time of the oscilloscope. The value of the resistor (10 MΩ) was determined to avoid a current flowing from the DC high-voltage source at the moment of the discharge occurring.

The way how the beginning of discharge is detected is described as follows:

1. When a discharge occurs, the field sensor and the current sensor detect the discharge field and the discharge current, respectively.
2. Output signal from either the field sensor or the current sensor is divided between two signals by the power divider shown in Figure 1.
3. One signal propagates through a delay line and is amplified by the main amplifier.

***Corresponding author:** Ishigami S, Professor, Faculty of Engineering, Tohoku Gakuin University, Japan, Tel: +81-22-368-7103; E-mail: shinobu@mail.tohoku-gakuin.ac.jp

Received July 05, 2017; **Accepted** August 28, 2017; **Published** September 04, 2017

Citation: Ishigami S, Kawamata K, Minegishi S (2017) Measurement and Consideration of the Breakdown Voltage in a Micro Gap ESD. J Biomed Syst Emerg Technol 4: 114.

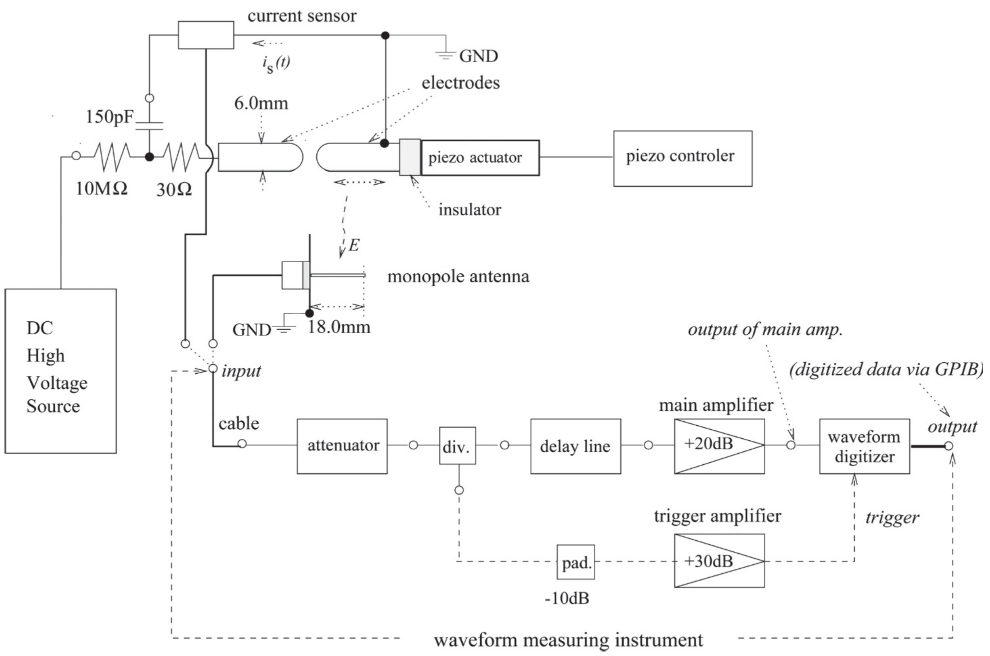

Figure 1: Experimental setup for measurements.

4. The other signal goes to the trigger amplifier and is used for a trigger.
5. The waveform digitizer starts to measure at about 45 ns later when the signal arrives into the trigger- input port of the digitizer. This is the reason that the delay line is used.

Therefore, the time of "0" in measured waveforms is the beginning time of a measurement by the waveform digitizer. The structure of the current sensor and the electric-field sensor are shown in Figure 2. A small monopole antenna is used as the electric-field sensor. The distance between the field sensor and the gap of the electrodes is 50.0 mm.

Measurement conditions

Waveforms of the discharge current and the electric field are measured in both cases where the discharge electrodes are fixed and where the electrode is approaching to the other electrode in speed of 1.71 μm/s using the piezo actuator. In the measurements, the gap length dg and the applied voltage Vs are changed as parameters. In the measurements, the gap length dg and the applied voltage Vs are changed as parameters. These waveforms are also measured in case of the approaching electrode whose speeds are from 8.4 cm/s to 33.6 cm/s by using the experimental setup shown in Figure 1. In this case, the right electrode is installed on a movable optical stage. A support of the discharge apparatus with the electrode can be moved manually on the movable optical stage. These speeds are determined by human movements. These speeds are determined by human movements. Through all measurements, discharges are performed in air and air pressure p0 is set to about 760 Torr (101.3 kPa).

In the fixed-electrodes experiment, the gap length is fixed, and a DC high-voltage is applied to the gap. A magnitude of the voltage is set higher than the voltage at which a discharge may occur. Next, the applied voltage is changed smaller gradually. The minimum applied voltage is determined as the discharge voltage at the gap length where discharge occurs.

In the approaching electrode, fixed DC high-voltage is applied, and the gap length decreases by the piezo actuator. The gap length when the discharge occurring is measured with the calibrated piezo actuator. This is the gap length for the given applied voltage.

Outputs detected by the field sensor and observed by the measuring instrument are involved the characteristics of the sensor and the instrument. Therefore, the actual field waveform should be obtained by reconstruction from the measured output by factoring out the characteristics of the sensor and of the instrument [6]. The sensor characteristic in frequency domain is expressed as the Complex Antenna Factor (CAF) [7], in which the phase information is added to the conventional antenna factor. The characteristics of the instrument are expressed in S-parameter in frequency domain.

The antenna factor and the complex antenna factor of a monopole antenna or a dipole antenna come into infinity when a frequency decreases toward zero. Therefore, we introduce a quantity of $j\omega F_c$, where ω is an angular frequency and F_c is the complex antenna factor. The term of *jω* corresponds to a time-derivative term in time domain. Measured $j\omega F_c(\omega)$ of the monopole antenna used as the field sensor is shown in Figure 3. In the figure, a low frequency of $j\omega F_c$ does not go toward infinity. A value of $j\omega F_c$ (ω=0), which is the value in a case where angular frequency is zero, is interpolating using the values of $j\omega F_c$ at the frequencies from 10 MHz to 100 MHz. The values of $j\omega F_c$ can be measured by the 3-antenna method [7].

A waveform of the electric field *E(t)* is reconstructed by using $j\omega F_c$ as [8]:

$$E(t) = \int_0^\infty F^{-1}\left[j\omega F_c(\omega)\frac{F\{v_s(t)\}}{s_{21}(\omega)}\right]dt \qquad (1)$$

where $v_s(\omega)$ is an output voltage of the waveform measuring instrument. $F\{\}$ and $F^{-1}\{\}$ denote the Fourier transform and the inverse Fourier transform, respectively. A waveform of the discharge current is $i_s(t)$ is also reconstructed as:

Citation: Ishigami S, Kawamata K, Minegishi S (2017) Measurement and Consideration of the Breakdown Voltage in a Micro Gap ESD. J Biomed Syst Emerg Technol 4: 114.

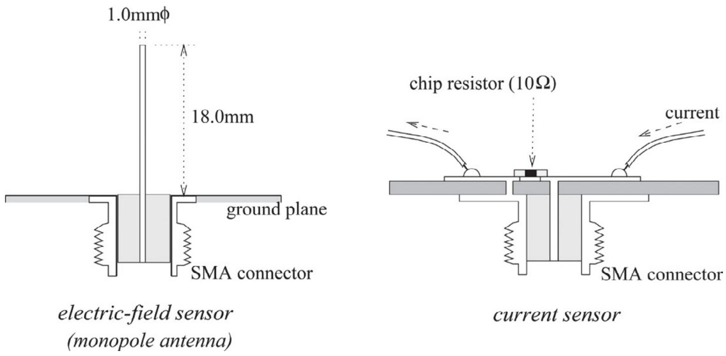

Figure 2: Structure of the current sensor and the electric field sensor.

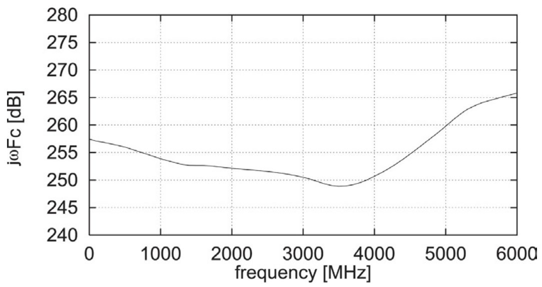

Figure 3: *jωFc* of the field sensor.

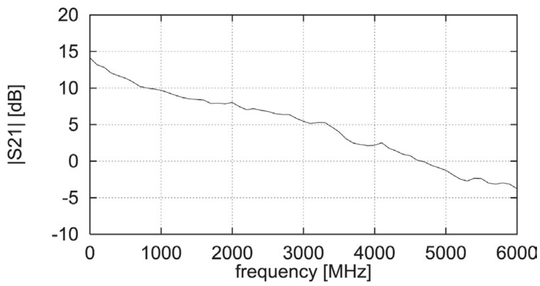

Figure 4: Measured *S*21(ω) of the waveform measuring instrument (Amplitude).

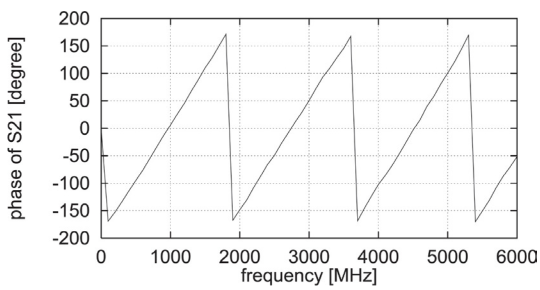

Figure 5: Measured *S*21(ω) of the waveform measuring instrument (Phase).

$$i_s(t) = F^{-1}\left[\frac{Z_0 + Z_s(\omega)}{Z_0 Z_s(\omega)} \cdot \frac{F\{v_s(t)\}}{S_{21}(\omega)}\right] \quad (2)$$

where Z_0 and $Z_s(\omega)$ are the characteristic impedance of the measurement instrument and the impedance of the current sensor, respectively. The term of $S_{21}(\omega)$ is defined as:

$$S_{21}(\omega) = S_{21p}(\omega) S_{21w}(\omega) \quad (3)$$

Where $S_{21p}(\omega)$ is the *S*-parameter denoting a transmission from the input of the instrument to the output of the main amplifier, and $S_{21w}(\omega)$ is the *S*-parameter denoting a transmission from the input to the output of the waveform digitizer as shown in Figure 1. The *S*-parameters S_{iis} (i=1,2 and s=p,w) are regarded as zero because it is considered that the reflections from the input and output ports of measurement instrument and from the input port of the waveform digitizer are quite small. $S_{21p}(\omega)$ is measured including a phase information by using a vector network analyzer. In a case of $S_{21w}(\omega)$ measurement, an input port of the waveform digitizer is connected with a CW signal generator. The output power of the generator P_{in} is measured by a power meter. The digitized sinusoidal-waveform is obtained by a personal computer (PC) via GPIB interface. $S_{21w}(\omega)$ is defined as:

$$S_{21}(\omega) = \frac{V_{out}}{\sqrt{P_{in} Z_0}} \quad (4)$$

Where V_{out} is the output voltage obtained from the measured waveform. The term of $S_{21w}(\omega)$ contains no phase information. The measured $S_{21}(\omega)$ is shown in Figures 4 and 5 (amplitude and phase).

Measurement of discharge current and field waveforms

Examples of measured discharge current waveforms are shown in Figures 6-9. In these figures, the time of "0" is the beginning of the measurement by the waveform digitizer. A discharge begins at the time denoted as "A" in each figure.

In Figure 6, the electrodes are fixed with the gap length of 3 μm and the applied voltage is 100 V, which is less than the minimum spark voltage provided by the Paschen's law (Paschen minimum). In a case where the gap length is set to 10 μm (Figure 7), the breakdown voltage is 370 V, which is more than the Paschen minimum. The Paschen minimum is around 330 V in air. The waveforms in Figures 6 and 7 contain a falling transition (from "A" to "B") at the initial discharge.

Figures 8 and 9 shows the waveforms in a case of the approaching electrode with applied voltages of 100 V and 400 V respectively. These discharges occur before the electrodes collide. Each waveform also contains the falling transition at the initial discharge.

Examples of measured electric-field waveforms are shown in Figures 10-13. The discharge begins at the time of "A" in these figures. A constant strength of electric field appears until the occurrence of discharge in each waveform, which is called as "quasi-electrostatic field". Immediately after the discharge, the field strength decreases

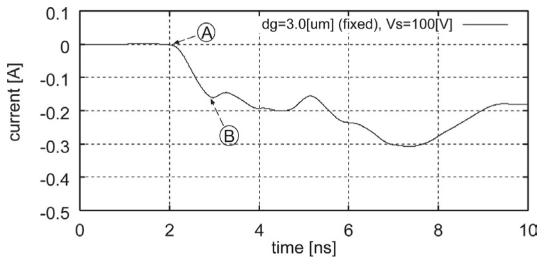

Figure 6: Measured discharge current (fixed electrode, *dg*=3 μm).

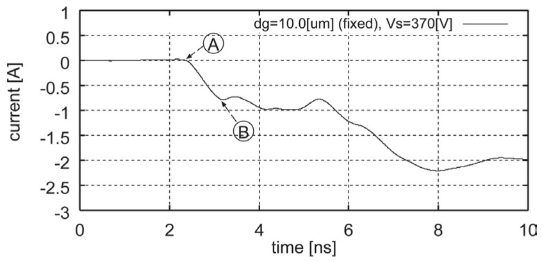

Figure 7: Measured discharge current (fixed electrode, *dg*=10 μm).

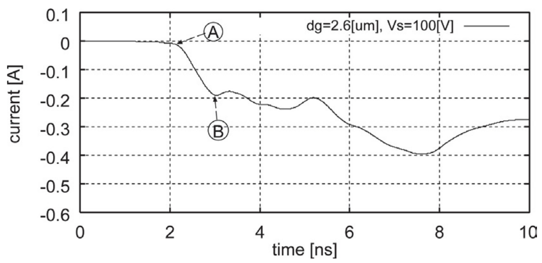

Figure 8: Measured discharge current (approaching electrode, *Vs*=100 V).

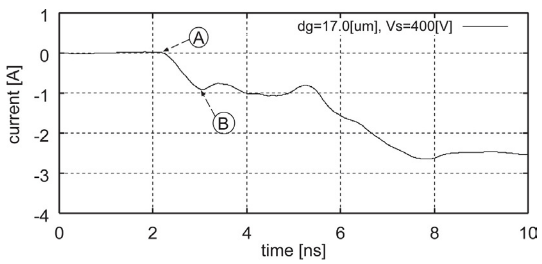

Figure 9: Measured discharge current (approaching electrode, *Vs*=400 V).

rapidly (from “A” to “B”) and the field decays with damped oscillation. Figures 10 and 12 show that a discharge occurs and an electric field is observed in a case where the applied voltage is less than the Paschen minimum. In these figures, the applied voltages are 150 V and 100 V, respectively.

There is a similarity of waveforms between the waveform at less and more than the Paschen minimum in the cases of discharge currents and electric fields. Wave shapes of the currents after the time of “B” may be due to the response of the circuit which is contained in the discharge apparatus (cables connected with the current sensor, the capacitor, and the resistors). The rise time of the initial discharge is not determined these lumped parameter elements, but is determined by the charge on two electrodes, an applied voltage to the electrodes, and a gap length between the electrodes. Ishigami and Iwasaki [9] describe the electric and magnetic fields radiated from the discharge instrument consist of two kinds of radiation. One radiation is from the gap immediately in a moment of the discharge. The radiation acts as the small electric-dipole. These fields will decay in time rapidly. The field results from the current generated by the neutralization of the initial static charges on the electrode. However, the current caused by the neutralization cannot be measured by such structure of the current sensor because the neutralization of the initial charges mostly occurs on the center of electrode, the current does not flow into the resistor of the current sensor. The rise time of the initial discharge is determined by the current. Another radiation is made from a current that flows through a mostly short-circuit path, which is made from the electrode, the current sensor, and the ground. The current of short-circuit path is provided by the lumped elements as shown in Figure 1.

Figure 14 shows strength of the “quasi-electrostatic field” for the applied voltage *Vs* until a discharge, where × and ○ denote in cases of the approaching electrode and the fixed electrodes, respectively. Solid line denotes the average of three times measurements at the same voltage in a case of the approaching electrode. In this figure, strength of the quasi-electrostatic field increases with the applied (breakdown) voltage except for the voltage range of nearby the Paschen minimum (300 V–400 V). It is not necessarily that the field strength is proportional to the applied voltage in a case of this voltage range.

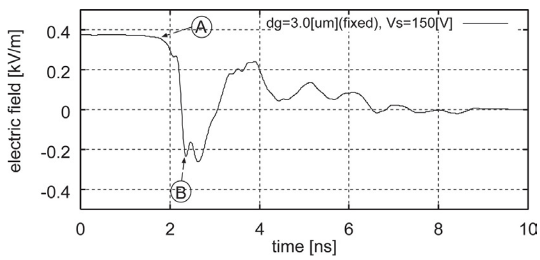

Figure 10: Measured electric field (fixed electrode, *dg*=3 μm).

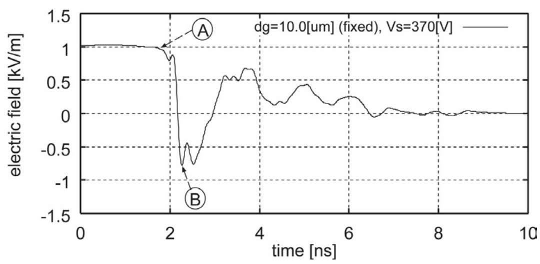

Figure 11: Measured electric field (fixed electrode, *dg*=10 μm).

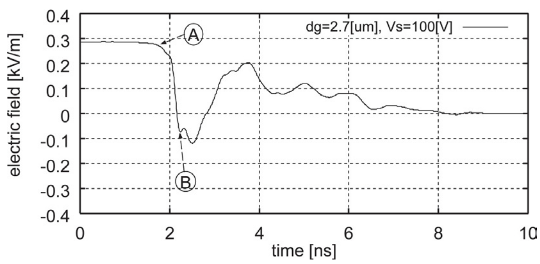

Figure 12: Measured electric field (approaching electrode, *Vs*=100 V).

Citation: Ishigami S, Kawamata K, Minegishi S (2017) Measurement and Consideration of the Breakdown Voltage in a Micro Gap ESD. J Biomed Syst Emerg Technol 4: 114.

Rise time of the transition (from “A” to “B”) of the initial discharge for each field-waveform is plotted to the applied (breakdown) voltage as shown in Figure 15, where × and ○ denote in cases of the approaching electrode and the fixed electrodes, respectively. Solid line denotes the average in a case of the approaching electrode. The rise time is defined as the time from 10 percent to 90 percent of the time difference between “A” and “B”. The rise time is the smallest in the range of the applied voltages from 200 V to 700 V, of which value is about 0.1 ns in both cases. When the applied voltage is less than 200 V and more than 700 V, the value of rise time is larger than the values at above voltage range. The result of reference [3] shows the same rise time of about 0.1 ns below 700 V. A reason for increasing of the rise time in the voltage range below 200 V is that a discharge except for a spark discharge may occur in a case of this voltage range.

The frequency range is limited when the reconstruction of the waveform is conducted because S21 of the waveform measuring apparatus and the complex antenna factor of the sensor have been measured with a frequency range of 6 GHz. It is a frequency limitation of a vector network analyzer which is used in the experiment. This limitation may be a cause that the smallest value of the rise time is 0.1 ns. If the frequency range is expanded more, there is possibility that the rise time may be smaller than this result.

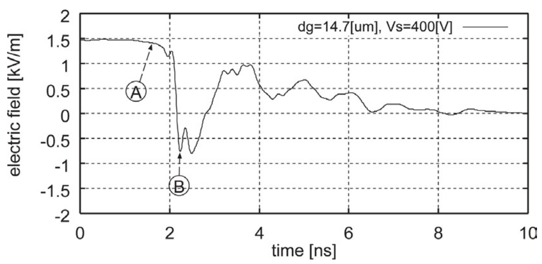

Figure 13: Measured electric field (approaching electrode, *Vs*=400 V).

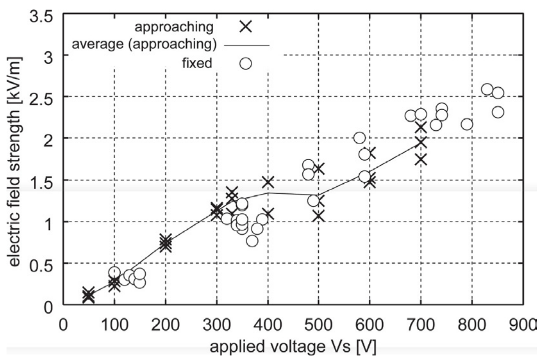

Figure 14: Strength of the “quasi-electrostatic field” to the applied voltage *Vs*.

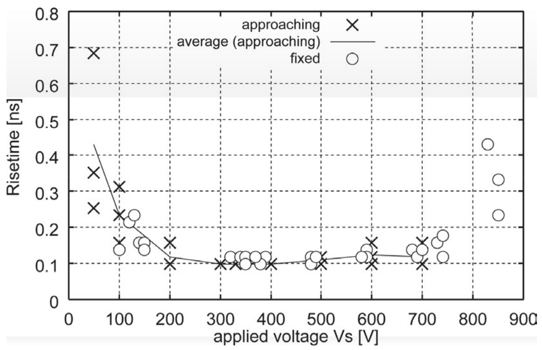

Figure 15: Rise time of the transition at initial discharge (electric fields).

The low-voltage ESD, especially below 700 V, may be most harmful to electronic equipment because a voltage induced on a print circuit board or a transmission line caused by an impulsive electromagnetic field is related with a rise time of the impulsive field.

Since the distance between the gap of the electrodes and the field sensor is 50 mm, the field at the observing point is in near-field zone. If the current source can be assumed to be a small electric dipole, the field contains not only the far-field component that is proportional to the time-derivative of current but also the near-field component that is proportional to the current and to an integral of the current. The rise times of the fields are smaller than those of currents as shown in Figures 6-9. The rise time of these currents is approximately 0.6 ns. Therefore, an evaluation of the induced voltage in a print circuit board cannot be easily carried out with only the assumption that the field is proportional to the time-derivative of the current.

Figure 16 shows that the strengths of the quasi-electrostatic fields measured by the apparatus are plotted for the applied voltage in cases where approaching speeds of the electrode are 0 cm/s (fixed), 8.4 cm/s, 16.8 cm/s and 33.6 cm/s. In this figure, the strength of the quasi-electrostatic field increases with the applied voltage. A difference depending on the approaching speed is not so large.

Figure 17 shows the rise time of the transition at the initial discharge in these electric fields. The approaching speeds of the electrode are the same values as those of Figure 16. The values of rise time are also about 0.1 ns in the whole of the applied voltage except for one approaching speed at 200 V. A reason for the results may be that these approaching speeds which correspond to a speed of human movements are far slower than the drift speeds of electrons and positive ions at a discharge [9].

Figures 18 and 19 (fixed electrode and approaching electrode) show the applied (breakdown) voltages Vs plotted for the gap lengths. In these figures, □ and Δ denote the measured *Vs-dg* characteristics of the electric field and of the discharge currents, respectively. Solid lines denote the *Vs-dg* curve that is calculated from the Paschen’s law [7] as follows:

$$V_s = \frac{B_2 p_0 d_g}{\log(A_2 p_0 d_g) - \log\left\{\log\left(1 + \frac{1}{\gamma_i}\right)\right\}} \tag{5}$$

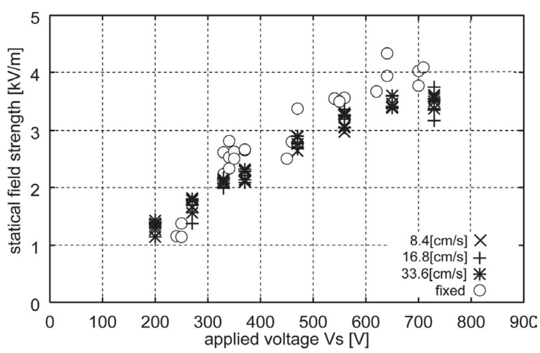

Figure 16: Strength of the “quasi-electrostatic field” to the applied voltage at approaching speed of 0 to 33.6 [cm/s].

Citation: Ishigami S, Kawamata K, Minegishi S (2017) Measurement and Consideration of the Breakdown Voltage in a Micro Gap ESD. J Biomed Syst Emerg Technol 4: 114.

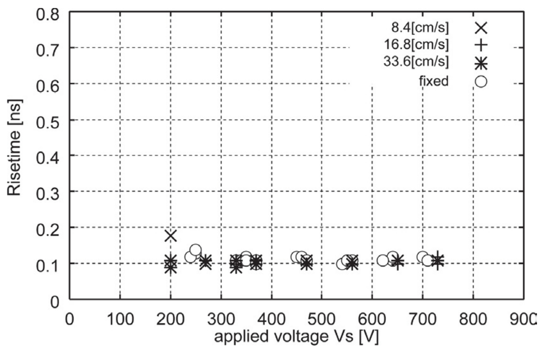

Figure 17: Rise time of the transition at initial discharge at approaching speed of 0 to 33.6 [cm/s].

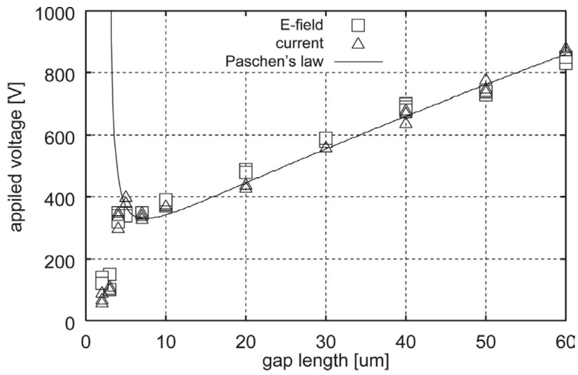

Figure 18: Applied (breakdown) voltage *Vs* to the gap length *dg* (fixed electrode).

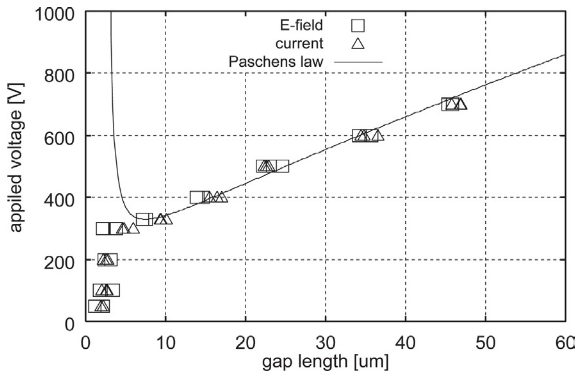

Figure 19: Applied (breakdown) voltage *Vs* to the gap length *dg* (approaching electrode).

Here A_2 and B_2 are constants, A_2=14.6 and B_2=582, respectively. And p_0 and γ_i are the pressure of gas [Torr] and the emission probability of electrons per one positive ion when the positive ion of air molecule rushes into the cathode, respectively. Value of γ*i* is determined as 0.05. These constants were obtained by experimental formula according to Masutani and Nakata [10].

In both of cases, fixed and approaching electrodes, the measured result agrees with the Paschen's curve in a case where the gap length is more than 4 μm. When the gap length is less than 4 μm, a discharge occurs below the Paschen minimum. The Paschen's law cannot apply to a discharge in a case of the gap length of less than 4 μm and in this case the breakdown voltage seems to be in proportion to the gap length.

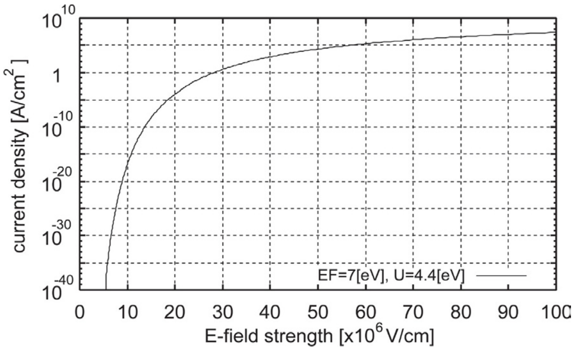

Figure 20: Current density of the field electron emission.

The breakdown voltages of the discharge current do not agree strictly with those of the E-field in the same gap length. A reason of the disagreement is that the discharge current and the electric field cannot be measured at the same time because the waveform digitizer only has one input port. Then, discharge conditions are different between the current measurements and the electric-field measurements. Humidity, temperature, soot on the electrode by the burned dust in air, and so on, are the discharge conditions.

Breakdown Model of Very-Small Gap Discharge

Let us consider a reason that the conventional Paschen's law cannot apply to the discharge in the gap length below 4 μm.

The conventional Paschen's law

Townsend's sparking criterion is given as follows:

$$\alpha d_g = \log\left(1+\frac{1}{\gamma_i}\right) \tag{6}$$

Here α is the coefficient of ionization by collision of electrons. Left of (6) is transformed as:

$$\frac{\alpha}{p_0} p_0 d_g = \log\left(1+\frac{1}{\gamma_i}\right) \tag{7}$$

Considering the relationship between α and the electric field *E*, the three experimental equations are proposed according to a value of *E*/*p*0 as follows [9]:

$$\frac{\alpha}{p_0} = A_1\left(\frac{E}{p_0} - B_1\right)^2 \tag{8}$$

$$\frac{\alpha}{p_0} = A_2 e^{\frac{B_2 p_0}{E}} \tag{9}$$

$$\frac{\alpha}{p_0} = \left(A_3\sqrt{\frac{E}{p_0}} - B_3\right) \tag{10}$$

where A_1, A_2, A_3, B_1, B_2, and B_3 are constants to determine the relationship between α/*p*0 and *E*/*p*0. These constants were obtained by experimental formula according to Ref. [9]. Equations (8)-(10) are used when *E*/*p*0 is small, middle and large, respectively.

The Paschen's law is derived from (7) and (9). Equation (7) is transformed by using (9) as

$$A_2 e^{-\frac{B_2 p_0}{E}} p_0 d_g = \log\left(1+\frac{1}{\gamma_i}\right) \tag{11}$$

When the electric field is uniform, the following equation holds.

$$\frac{E}{p_0} = \frac{V_s}{p_0 d_g} \tag{12}$$

From (11) and (12), *Vs* is expressed as

$$V_s = \frac{B_2 p_0 d_g}{\log\left(A_2 p_0 d_g\right) - \log\left\{\log\left(1+\frac{1}{\gamma_i}\right)\right\}} \tag{13}$$

Equation (13) is led as the equation of the Paschen's law.

Breakdown model at high strength electric-field

Term of α at high strength electric-field: In Raizer and Allen [11], the Paschen's law is applicable under the conditions as follows:

- p_0: 10-2–2400 Torr.
- d_g: 5 μm–20 cm.

Moreover, a proper range of (9) is *E*/*p*0 =150–600 V/cm·Torr in air.

In this experiment, the range of *E*/*p*0 in a case where the gap length *d*g is below 4 μm is about 400–1800 V/cm· Torr, where the air pressure is 760 Torr.

Since the gap length deviates from the applicable range for the Paschen's law and the values of *E*/*p*0 in the experiment is larger than the proper range of (9), we try to derive the breakdown voltage *Vs* from (10). Equation (10) is the experimental equation of α when an electric-field strength is higher than that those for (9). *Vs* can be obtained from (7) and (10) as

$$V_s = \left\{\frac{\log\left(1+\frac{1}{\gamma_i}\right)}{A_3 p_0 d_g} + B_3\right\}^2 p_0 d_g = \frac{c^2}{p_0 d_g} + 2CB_3 + B_3^2 p_0 d_g \tag{14}$$

Where

$$C = \frac{\log\left(1+\frac{1}{\gamma_i}\right)}{A_3} \tag{15}$$

Equation (14) is under an assumption that the discharge can be explained by the breakdown model.

Influence of field electron emission: Next, let us examine whether a field electron emission occurs or not on above high-strength electric-field. Current density *jF* A/cm² by a field electron emission is calculated by the Fowler-Nordheim formula [12] as:

$$j_F = 6.2\times10^{-6}\frac{\sqrt{\frac{E_F}{U}}E^2}{E_F+U}e^{-\frac{6.85\times10^7 U^{1.5}\xi}{E}} \tag{16}$$

where *EF* [eV] is the Fermi energy, *U* [eV] is the work function, ξ is a correction factor, and *E* is electric field given in V/cm. Figure 20 shows calculated current density of the field electron emission from a copper electrode in conditions of *EF*=7[eV], *U*=4.4[eV] and ξ=0.9 [12].

When E/p_0 is 1800 V/cm·Torr at *p*0=760 Torr, the electric-field strength is 1.368×10^6 V/cm. The current density at this field strength is smaller than 10^{-40} A/cm² from this figure. By the way, field strength in a case where the current density is 1 A/cm² is about 2.8×10^7 V/cm in this case.

This result is the evidence that effect of the field electron emission may be quite small in the experiment. We also calculate a current density *jT* caused by the thermionic emission [12]. As a result, *jT* is calculated as about 1.27×10^{-67} at the temperature of electrodes T=300 [K]. This effect also can be ignored. Therefore, we can consider that the discharges in the experiment may be explained by the breakdown process.

Breakdown process in high-strength electric-field

We assume that the coefficient α is simply a function of the electric field *E*, and an air pressure is about 760 Torr and a type of gas is air in this paper.

Many references, for example [12], do not mention the experimental results of α/p_0 in air in a case where E/p_0 is more than 1000 V/cm·Torr. A value of E/p_0 where the current density of field electron emission becomes 1 A/cm² is about 3.68×10^4 V/cm· Torr. A range of E/p_0 where the discharge occurs below the Paschen minimum in the experiment is about 400–1800 V/cm·Torr. The characteristics of α/p_0 in E/p_0 of more than 1000 V/cm·Torr need to be unraveled in order to explain the breakdown process in above range of E/p_0.

The coefficients A_3 and B_3 in (10) that is used in above section are given as 0.4 (V·cm·Torr)-0.5 and 6.62 [V/(V·cm·Torr)$^{0.5}$], respectively [12]. A value of the coefficient γ*i* is in a range from 0.1 to 0.01 according to Raizer and Allen [12]. Here γ_i is assumed as 0.05. Then, the value of *C* in (14) is calculated from (15) as 7.61. Using these values and (14), the characteristic curve of the breakdown voltage V_s for the gap length d_g as shown in a dashed curve of Figure 21 is obtained. However, this curve does not trace the result of measurement (Δ in the figure).

The values of E/p_0 at $d_g \le 4$ μm in the measurement result are mostly beyond 1000 V/cm·Torr. Then, it is assumed that a dependency of α for the electric field increases in the range of high-strength electric-field. Equation (10) is not changed on this assumption. The strength of the electric fields increases as the velocities of electrons may increase. Molecules that are possible to ionize exist sufficiently in a case where the air pressure is 760 Torr. The velocities and the quantities of positive ions may also increase.

Evaluating from the measurement result, A_3 and B_3 are calculated as 2.4 and 26, respectively. Since both numbers of α and electric-field strength increase, the number of the positive ions which rushes into the cathode increases. Then it is assumed that the value of γ_i is twice as much, i.e., γ_i =0.1. The breakdown voltage is calculated by using these

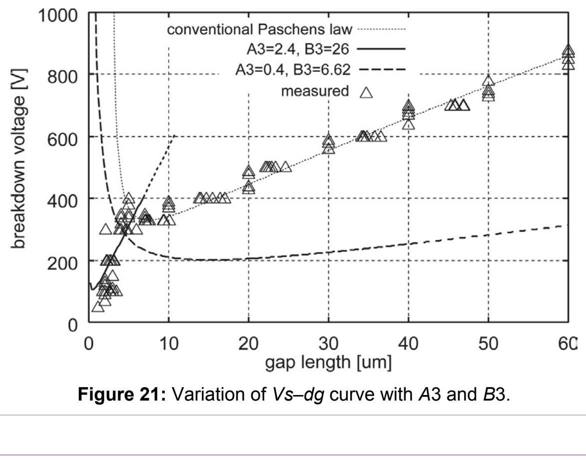

Figure 21: Variation of *Vs–dg* curve with *A*3 and *B*3.

values and (14). The characteristic curve of the breakdown voltage for the gap length as shown in a solid curve of Figure 21 is obtained. This curve traces near the result of measurement.

Figure 22 shows the variation of α/p_0 for E/p_0 in cases where A_3 and B_3 are 2.4 and 26 (solid line) and A_3 and B_3 are 0.4 and 6.63 (dashed line), respectively. The solid line and the dashed line cross at around E/p_0=890 V/cm·Torr and α/p_0 is about 9.2 (V·cm·Torr)$^{-1}$ at the point. In the range near the point, α/p_0 may vary smoothly shown like a thin-dotted line shown in this figure.

If Equation (10) is applicable in the range of E/p_0 where (9) is usable, A_3 and B_3 are calculated using A_2 and B_2 as0.48 and 12.94, respectively. Figure 23 shows V_s–d_g curves calculated by using (14) in cases where A_3=2.4, B_3=26, γ_i =0.1 and C=1 (solid line) and A_3=0.48, B_3=12.94, γ_i =0.05 and C=6.34 (dashed line). Dotted line denotes the characteristic curve drawn in the conventional Paschen's law. The dashed line agrees with the result of measurement in a case where the gap length is more than 4 μm. The solid line agrees with the result of measurement at the gap length of less than 4 μm.

Therefore, the breakdown process can be explained in terms of only (14) under the assumption that the relationship between the coefficient α and the electric field is expressed by (10). Then the values of A_3 and B_3 vary with strength of the electric field. Equation (14) expresses the Paschen's law in a case where a value of B_3 is almost comparable to C and explains the breakdown below the Paschen minimum in a case where B_3 is far larger than C.

Conclusion

We examined that the physical processes of an electrostatic discharge occurring on the applied voltage of less than 330 V and at gap lengths of several micrometers by measuring the discharge current and electric fields. As a result, it was confirmed that the conventional Paschen's law cannot be applied to the characteristics of discharges on the applied voltage of less than 330 V in the gap lengths of less than 4 μm in both cases of approaching electrode and fixed electrode. The breakdown process was explained in terms of the equation describes the relationship between high density electrons and electric-field strength that is applied for high electric-field. The proposed equation expressed both the conventional Paschen's law and the breakdown process below the Paschen minimum.

In future work, it should be examined that the breakdown process is applicable or not for various types of gas and pressure.

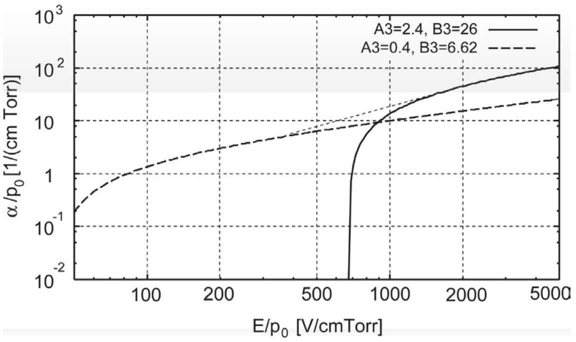

Figure 22: Variation of α/*p*0 with the value of *A*3 and *B*3.

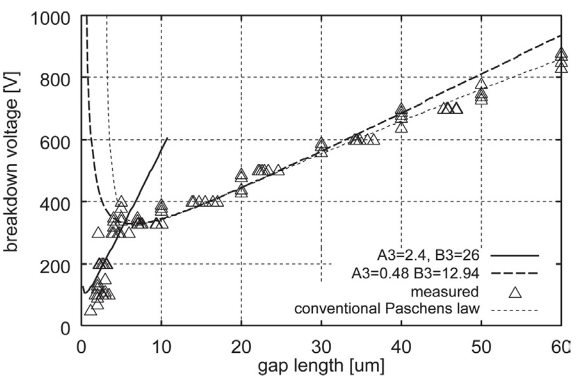

Figure 23: *Vs–dg* curve calculated by Eqn. (14).

Acknowledgment

The authors would like to thank Prof. Takashi Iwasaki, emeritus professor of the University of Electro- Communications, for his support and helpful suggestions.

References

1. Honda M (1990) Indirect ESD measurement using a short monopole antenna. 1990 IEEE International Symposium on Electromagnetic Compatibility: 641-645.
2. Honda M (1989) A new threat-EMI effect by indirect ESD on electronic equipment. IEEE Transactions Industry App 25: 939-944.
3. Kawamata K, Minegishi S, Haga A, Sato R (1999) A measurement of very fast transition durations due to gap discharge in air using distributed constant line system. IEEE T Electromagn C 41: 137-141.
4. Bock K, Hartnagel HL (1992) New field-emitter switch for ESD protection of microwave circuits. Electron Lett 28: 1822-1824.
5. Torres J, Dhariwal RS, King PC (1999) Electric field breakdown at micrometre separations in various media. In High Voltage Engineering. Eleventh International Symposium. 3: 201-204.
6. Ishigami S, Gokita R, Nishiyama Y, Yokoshima I, Iwasaki T (1995) Measurements of fast transient fields in the vicinity of short gap discharges. IEICE Trans Commun 78: 199-206.
7. Ishigami S, Iida H, Iwasaki T (1996) Measurements of complex antenna factor by the near-field 3-antenna method. IEEE T Electromagn C 38: 424-432.
8. Sugiura A, Kuwabara N, Iwasaki T (1997) Current topics of microwave EMI antennas and measurements. IEICE Trans Commun 80: 653-662.
9. Ishigami S, Iwasaki T (1996) Evaluation of charge transition in a small gap discharge. IEICE Trans Commun 79: 474-482.
10. Masutani T, Nakata J (1980) High voltage engineering, Corona pub.
11. Handbook of Electrostatics (1981) Ohm-sha.
12. Raizer YP, Allen JE (1997) Gas discharge physics. Berlin: Springer.